

Acoustic and magnetic wave heating in stars

II. On the range of chromospheric activity

D. Fawzy¹, P. Ulmschneider¹, K. Stępień², Z. E. Musielak^{3,1}, and W. Rammacher¹

¹ Institut für Theoretische Astrophysik der Universität Heidelberg, Tiergartenstr. 15, 69121 Heidelberg, Germany

² Warsaw University Observatory, Al. Ujazdowskie 4, 00478 Warszawa, Poland

³ Department of Physics, University of Texas at Arlington, Arlington, TX 76019, USA

Received 10 October 2001 / Accepted 18 February 2002

Abstract. In the first paper of this series we developed a method to construct theoretical, time-dependent and two-component chromosphere models for late-type main sequence stars. The models consist of non-magnetic regions heated by acoustic waves and magnetic flux tube regions heated by magnetic tube waves. By specifying the magnetic filling factor, theoretical models of stellar atmospheres with different chromospheric activity can be calculated. Here, these models are used to simulate the emerging Ca II and Mg II chromospheric emission fluxes and compare them with observations. The comparison shows that the wave heating alone can explain most but not all of the observed range of chromospheric activity. In addition, the results obtained clearly imply that the base of stellar chromospheres is heated by acoustic waves, the heating of the middle and upper chromospheric layers is dominated by magnetic waves associated with magnetic flux tubes, and that other non-wave (e.g., reconnective) heating mechanisms are required to explain the structure of the highest layers of stellar chromospheres.

Key words. methods: numerical – stars: chromospheres – stars: coronae – stars: magnetic fields – MHD – waves

1. Introduction

In the first paper of this series (Fawzy et al. 2002, henceforth called Paper I), a method was developed to construct theoretical models of stellar chromospheres and simulate total emission fluxes in Ca II H and K lines and Mg II h and k lines emerging from these models. The main aim of this paper is to use these models to determine theoretical range of chromospheric activity for late-type dwarfs and compare it with observations (see also Ulmschneider et al. 2001a).

The fact that stars of the same spectral type and gravity show a broad range of chromospheric activity has been well-established by numerous ground and space observations (e.g., Vaughan & Preston 1980; Noyes et al. 1984; Rutten 1987; Stępień 1993). This variation of the chromospheric activity is attributed to different stellar rotation rates, which determine the coverage of the stellar surface by magnetic fields. The simple dynamo theory predicts that rapidly rotating stars should possess significantly stronger magnetic fields than slow rotators (e.g. Durney & Latour 1978).

The observations of chromospheric activity are in agreement with these predictions and indeed the activity

is most prominent in rapidly rotating stars and decreases with lower rotation rates (Noyes et al. 1984; Rutten 1987; Stępień 1994; Strassmeier et al. 1994). For the slowest rotators, a minimum chromospheric line core emission has been observed (Wilson 1968; Schrijver 1987; Rutten et al. 1991; Strassmeier et al. 1994). On the other hand, the most rapid rotators show a maximum amount of the line core emission (Vilhu 1987; Vilhu & Walter 1987). Direct measurements of stellar magnetic fields also show an increase of the photospheric magnetic flux with increasing rotation rate (Saar 1994, 1996). As a result, a strong correlation exists between calcium emission flux and the observed magnetic filling factor, which is defined as the ratio of the stellar surface area permeated by magnetic fields to the total surface area. This was first found by Schrijver et al. (1989) for solar active regions and later shown to hold also for stars over a broad range of activity by Stępień (1994).

Since the stars are uniquely described by four basic parameters, namely, effective temperature T_{eff} , gravity g , metallicity Z_{M} and rotation period P_{rot} , the main theoretical challenge is to understand the observed range of stellar activity in terms of these four parameters. As already mentioned in Paper I, two basic and currently unsolved theoretical problems naturally arise. The first is to predict theoretically the distribution of magnetic fields on

the surface of a star with known rotation rate. This requires a first-principle theory of stellar dynamos, which is not yet available (e.g. Weiss 1994). The second is to identify the basic physical processes which are responsible for the heating of stellar chromospheres and explain the observed range of stellar chromospheric activity in terms of the magnetic field coverage. Our aim here is to address the second problem by constructing theoretical chromospheric models based exclusively on wave heating (see Paper I) and using them to predict the magnitude and range of the chromospheric emission activity in stars with different magnetic filling factors. In our theoretical models, the magnetic filling factor formally replaces the stellar rotation rate, P_{rot} , and is treated as a free input parameter. Hence, the models are uniquely determined by specifying T_{eff} , g , Z_M , and the magnetic filling factor f at the stellar surface.

A series of theoretical chromospheric models for late-type dwarfs is computed and the emission fluxes in Ca II H and K lines and Mg II h and k lines emerging from these models are calculated. The results obtained are then used to determine the theoretical range of chromospheric activity and compare it with observations. In addition, based on the results obtained, we are able to determine the role played by acoustic and magnetic waves in the heating of chromospheres of late-type stars with different level of activity. Our paper is organized as follows: Sect. 2 describes the observational evidence for the minimum and the maximum flux limits of the chromospheric activity; Sect. 3 presents our theoretical emission flux simulations and comparison of these results to observations; and our conclusions are given in Sect. 4.

2. Observational data

To test our theoretical predictions (see Sect. 3), reliable observational data on chromospheric losses in the emission cores of Ca II H and K lines as well as Mg II h and k lines are needed. Particularly important, from our point of view, are the observations of the most active and least active stars, which define an upper and lower boundary of the chromospheric activity in the emission flux versus colour diagram. There exists a large volume of data in the literature on radiative losses in calcium and magnesium lines. Unfortunately, a number of different reduction and calibration procedures have been used, which make a direct comparison of absolute chromospheric fluxes difficult. Some of these fluxes contain significant systematic errors, for instance because of the photospheric background fluxes, which for calcium can be by factors of five larger than the chromospheric fluxes.

The Mg II observations suffer much less from these problems. They all have been obtained spectroscopically (mostly with IUE) and the photospheric flux in the investigated stars is small or negligible around the region of 2800 Å, compared to the chromospheric flux. Other uncertainties of the chromospheric fluxes may arise from the conversion of apparent fluxes to stellar surface fluxes (see

Sect. 2.2 below). However, this should not increase substantially the total error of the Mg II fluxes, estimated at 30% (Dupree et al. 1990).

The bulk of calcium emission flux data in the literature has been obtained with the Mt. Wilson photometer. However, different reduction and calibration procedures adopted by various groups and (in some cases) numerous revisions of the used constants result in a highly inhomogeneous material on the stellar fluxes. This prompted us to newly reduce the photometric observations of extreme activity stars, by using a uniform reduction and calibration procedure, based on the most recent investigations, of which below a critical review is given. Particular care has been given to assure agreement with the spectroscopically observed fluxes.

For the photometric as well as spectroscopic observations the reduction procedure consists of three basic steps: the measurement of the core flux in the instrumental system, subtracting the flux of non-chromospheric origin and converting the chromospheric flux into absolute units. The first step is relatively straightforward and indisputable. For spectroscopic observations it requires measuring the flux in a 1 Å or 2 Å band centered on the line core and expressing it relative to the nearby continuum, i.e. calculating the equivalent width. In case of a photometric measurement an index S is formed, containing essentially the same information. Significant differences appear when the second and third step are implemented by different authors. We now discuss these steps in more detail.

2.1. Non-chromospheric contribution to the observed calcium emission lines

The problem of separating the activity related flux from the non-chromospheric component was already discussed by Wilson (1968). After plotting the observed flux versus the $b - y$ index he noticed a clear lower limit to the observed flux, which is a function of colour. He suggested that this minimum flux should be subtracted from the observed flux of each star and the resulting flux should be a measure of the chromospheric activity. He realized, nevertheless, that the minimum flux may still contain some amount of the chromospheric flux. His idea was further developed by the Utrecht group (see below).

Blanco et al. (1974) have proposed that the flux of non-chromospheric origin in the core can be determined by extrapolating the absorption line wings into the core and subtracting the thus obtained background flux from the observed flux. Some of the spectroscopic observations made by the Italian group have been reduced in this way. Later, Linsky et al. (1979) presented a more elaborated approach. They used model atmospheres in radiative equilibrium to obtain the core flux of purely photospheric origin. The resulting fluxes were plotted for different stars versus the $V - R$ index and connected by a smooth relation. Their results show that both the Wilson minimum flux and the Blanco et al. flux overestimate the non-chromospheric

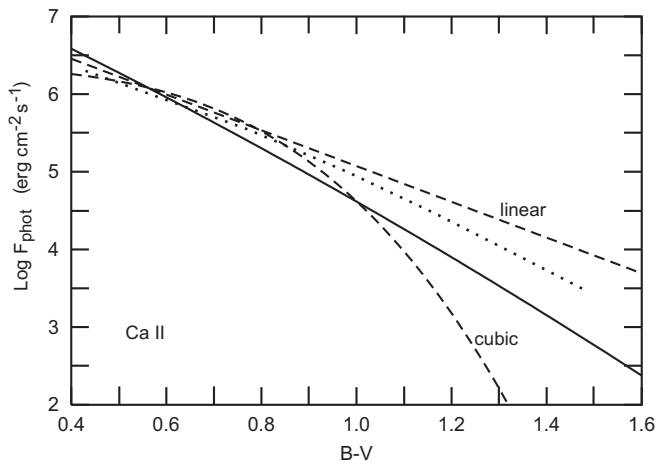


Fig. 1. Photometric flux in the observed cores of Ca II H and K lines, after Dupree et al. (1999) (solid), Noyes et al. (1984) (dashed) and Linsky et al. (1979) (dotted).

flux thus underestimating the chromospheric contribution. Since then, Linsky et al.'s photospheric flux has been frequently used to reduce the spectroscopic observations of Ca II H and K lines.

A large number of stars have been observed photometrically at the Mt. Wilson Observatory using the photometer built by Olin Wilson and resulting in an S index. The procedure to obtain absolute fluxes from the photometric S index was described by Noyes et al. (1984). Because of the triangular passband of the filter with $FWHM$ equal to 1.09 \AA , some light from the line wings (outside of the K1 and H1 minima) leaks into the photometer. Noyes et al. (1984) estimated the amount of the photospheric flux in the line wings from high dispersion spectrograms of a few stars and the Sun and they derived a cubic relation in $B - V$ (they also give another, linear relation in the same paper, see Fig. 1). They argued, on the other hand, that due to a nonlinear response of the atmosphere to the chromospheric temperature rise, the best assumption is to adopt zero for the core photospheric flux.

Mewe et al. (1981) and Schrijver (1983) revived the idea of Wilson (1968) and argued that the empirically determined minimum flux (defined as a lower limit to the observed flux plotted versus colour) should be subtracted from each observed flux to obtain the activity related chromospheric excess flux. The coronal X-ray flux correlates best with the excess calcium emission flux determined in this manner. Schrijver (1987) suggested that this lower limit, called “basal” flux, describes pure acoustic heating, independent of the level of magnetic activity. An obvious disadvantage of the use of such an empirical limit is that it depends on the sample of stars used to derive it. As a result, the “basal” flux was revised several times by the Utrecht group. Moreover, as had been shown by Linsky et al. (1979), the “basal” flux still contains a photospheric component. This was admitted by Rutten et al. (1991) who gave not only the revised values of the “basal” flux for calcium and magnesium lines (their Table 5 and Fig. 1)

but also the values of the “true basal” flux (basal flux minus photospheric flux) in Sect. 6.2 and Fig. 5 of the same paper.

Recently, a thorough analysis of the radiative losses in calcium emission lines of the M 67 giants was carried out by Dupree et al. (1999). Using Kurucz model atmospheres for giants they determined the photospheric contribution to the Mt. Wilson photometer passband. After plotting F_{phot} versus $B - V$ they derived a smooth polynomial relation for the background flux.

Figure 1 summarizes the above discussion on the photospheric flux. The $F_{\text{phot}}(B - V)$ relations of Noyes et al. (1984) and Dupree et al. (1999) are taken directly from their papers, and the relation by Linsky et al. (1979) was transformed from $V - R$ to $B - V$, using the Johnson photometry.

A number of interesting conclusions can be drawn from the figure. For $0.4 \leq B - V \leq 0.8$ all relations are remarkably close to one another, differing at most by a factor of two at the edges of the interval. The differences are still within this limit for the values of $B - V$ up to about 1, except for the linear relation given by Noyes et al. (1984), which, however, does not seem to be often used. That means that no gross differences exist among the published chromospheric fluxes of stars (even inactive ones) with $0.4 < B - V < 1.0$ as long as they are determined with one of the plotted relations. This does not apply to the excess calcium emission fluxes from the Utrecht group because their “basal” flux is much higher than the plotted curves.

The discrepancies among different photospheric fluxes become appreciable only for the lowest activity red stars with total fluxes comparable to the photospheric flux. As the photospheric contribution becomes less and less important, the more active red stars get progressively less affected. Consider the limits of applicability of the plotted relations. Noyes et al. (1984) derived the cubic relation from stars with $B - V < 0.83$. They (and other authors) used this relation also for cooler stars, based on the assumption that the photospheric flux is unimportant for the red stars. But, as discussed above, this is not true for low activity stars. No information on applicability limits of the linear relation is given by Noyes et al. (1984) but it was probably derived from the same stars.

On the other hand, the relations given by Linsky et al. (1979) and Dupree et al. (1999) are based on stars up to M spectral type, so they can be used over the whole interval of $B - V$ plotted in Fig. 1. They agree with one another quite well but they do not agree with the extrapolation of the relations given by Noyes et al. (1984). We conclude that the chromospheric calcium emission fluxes of low activity red stars can be significantly over- or underestimated, depending on whether the extrapolated cubic or linear relation for F_{phot} given by Noyes et al. (1984) was used. Here, we adopt the relation given by Dupree et al. (1999) because it is based on the more recent Kurucz model atmospheres and was used for the Mt. Wilson photometer passband with which the great majority of

inactive and very active stars discussed in this paper were measured.

2.2. Conversion of the chromospheric flux into absolute units

Two main methods of the conversion of apparent fluxes into stellar surface fluxes have been used. The first assumes that the conversion factor is inversely proportional to the stellar angular diameter and uses the Barnes-Evans relation for stellar radii, while the second assumes that the conversion factor is proportional to the ratio of bolometric flux on the stellar surface to the apparent bolometric flux. Mathioudakis & Doyle (1992) reduced the observations of several K and M stars using both methods and found differences in the absolute fluxes reaching 50%. In a few cases differences reached even a factor of two. Here, we adopt the later method introduced by Middelkoop (1982), which is in common use by the authors reducing the Mt. Wilson photometric measurements, but we are aware of an existing uncertainty of the chromospheric fluxes resulting from this conversion.

Apart from the conversion problem of the apparent flux into the surface flux, a numerical constant converting the absolute flux into physical units is necessary. Recently Hall & Lockwood (1995) presented a detailed discussion of the method of its determination and of the several revisions suggested in the literature (up to about twice its original value – see also Stępień 1989). The authors re-determined its value and showed that it gives now fully consistent results when applied to photometrically measured bright, nearby stars, to the stars observed by Linsky et al. (1979) and to the Sun. Fortunately, their value turned out to be close to the one given by Middelkoop (1982) and used, among others, by Noyes et al. (1984) which means that the fluxes obtained by these authors do not need to be revised. We adopted the value given by Hall & Lockwood (1995) when reducing the observations.

2.3. Our sample of high and low activity stars

We searched the literature for stars with extreme (very low, or very high) chromospheric activity. The main source of the data was the extensive list of over 65 000 measurements obtained with the Mt. Wilson photometer and published by Duncan et al. (1991). To find low activity stars, we selected stars with low values of the S index (allowing for its variation with colour) and reduced them, as discussed above. A few additional low activity stars were taken from Soderblom et al. (1991) and reduced similarly. Henry et al. (1996) observed H and K lines in a number of southern dwarfs using an echelle spectrograph. They developed their own reduction procedure but they calibrated the resulting net fluxes with the use of several Mt. Wilson stars so that their results are in a full

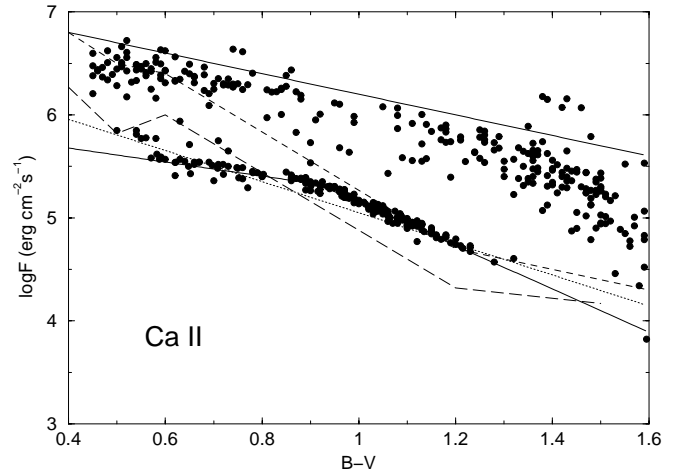


Fig. 2. Observed chromospheric calcium emission fluxes of low and high activity stars (filled circles). Solid lines mark approximate lower and upper limits on the observed fluxes. A lower limit on the fluxes of field giants (Strassmeier et al. 1994) is plotted as a dotted line. The “basal” flux and “true basal” flux, given by Rutten et al. (1991) are plotted as dashed and long-dashed lines, respectively.

agreement with the Noyes et al. (1984) data. We included their low activity stars in our list.

A few stars observed spectroscopically and showing very low levels of activity were taken from Strassmeier et al. (1990, 1994). Their fluxes agree very well with photometrically determined fluxes of low activity stars of the same colour. Three low activity M stars were taken from Mauas et al. (1997) and Doyle et al. (1998). The stars were observed spectroscopically and the authors used their own theoretical model atmospheres to determine the chromospheric flux. The star Gl 105B with $B - V \approx 1.6$ is a particularly important data point. As Doyle et al. (1998) point out, this is the least active M dwarf known. Members of several young open clusters and nearby stars from the Wooley catalogue, listed by Duncan et al. (1991), were taken as high activity stars and their observations were reduced by us. The values of $B - V$ colour for the investigated stars were taken from the *UBV Photoelectric Catalogue* by Mermilliod (1994) and the absolute calibration of $B - V$ in terms of effective temperature was taken from Flower (1996).

A number of measurements of the S index were rejected during the analysis. A few Hyades and Pleiades stars, measured on July 22, 1977, showed S values about an order of magnitude larger than on other nights. We rejected all of them (a couple of stars measured just only on that date were dropped from our sample altogether). The listed values of S for some stars resulted in too low observational fluxes – lower than the photospheric flux. This happened only for a few stars with just one measurement of S and relatively blue $B - V$ where the photospheric flux is much larger than the net flux of low activity stars. Such stars were also rejected.

The resulting absolute calcium emission fluxes of our stars are shown in Fig. 2. Taking into account all sources of possible errors and uncertainties we estimate very conservatively the overall accuracy of the plotted fluxes to about 30% for low activity stars and about 20% for high activity stars. It is seen that the minimum flux is quite well defined whereas the upper limit looks more ragged. A dense clump lying along the lower boundary, for $B - V$ between 0.85 and 1.25, consists mostly of giants, some of them observed spectroscopically (taking only main-sequence stars does not change much this limit, although the minimum flux is then less well defined in this range). The other data points in Fig. 2 correspond mostly to dwarfs. We find that approximate upper and lower limits for the observed fluxes are given by

$$\begin{aligned} \log F_{\max} &= 7.2 - (B - V), \\ \log F_{\min} &= 5.95 - 0.68(B - V), \quad 0.4 \leq B - V \leq 0.9, \\ \log F_{\min} &= 7.25 - 2.1(B - V), \quad 0.9 \leq B - V \leq 1.6. \end{aligned} \quad (1)$$

For comparison a lower limit on the calcium emission flux of field giants given by Strassmeier et al. (1994) is reproduced as a dotted line. The “basal” flux and the “true basal” flux from Rutten et al. (1991) are also plotted as dashed and long-dashed lines, respectively. Our lower limit agrees very well with the Strassmeier limit and reasonably well with the true basal flux. The “basal” flux curve appears to be too high.

3. Simulated theoretical emission fluxes

We now employ the methods described in Paper I to simulate theoretical emission fluxes. It has to be emphasized that *the theoretical calculations are based completely on first principles*, that is, we only specify the four independent stellar parameters: effective temperature T_{eff} , gravity g , metallicity Z_{M} (we took solar-like population I metal abundances) and magnetic filling factor f at the stellar surface. The selected main-sequence stars are listed in Table 1 (taken from Paper I), and the filling factors are assumed to vary between $f = 0$ and $f = 0.4$. With these four parameters, which uniquely identify a star, we constructed convection zone models and models of the magnetic flux tube forest which uniformly covers the stellar surface. Note that the clumping of flux tubes at the supergranulation boundaries and starspots are disregarded in this approach.

We assume that the magnetic field occurs mainly in the form of thin flux tubes, which at the stellar surface have diameters equal to the local scale height. The magnetic field strength at this height is assumed to be given by a fixed fraction of the equipartition field strength, which is determined by the external gas pressure.

Using the Lighthill-Stein theory (Lighthill 1952; Stein 1967) for the generation of acoustic waves in stellar

Table 1. Total propagating longitudinal tube wave fluxes F_{L} and acoustic fluxes F_{A} ($\text{erg cm}^{-2} \text{s}^{-1}$) for main-sequence stars of given spectral type, T_{eff} (K) and gravity (cm s^{-2}). Also given are the longitudinal P_{L} (s) and acoustic P_{A} (s) wave periods used for monochromatic wave calculations.

Star	T_{eff}	$\log g$	F_{L}	P_{L}	F_{A}	P_{A}
F5V	6440	4.34	1.1×10^9	85	6.7×10^8	55
G0V	6030	4.39	8.8×10^8	75	3.2×10^8	46
G5V	5770	4.49	5.6×10^8	63	1.7×10^8	42
K0V	5250	4.49	3.8×10^8	58	5.2×10^7	38
K5V	4350	4.54	1.1×10^8	54	3.8×10^6	34
M0V	3850	4.59	2.0×10^7	50	3.6×10^5	31

convection zones (Musielak et al. 1994; Ulmschneider et al. 1996) and a numerical method (Ulmschneider & Musielak 1998) for the generation of magnetic waves in stellar atmospheres (Ulmschneider et al. 2001b), we calculated acoustic and longitudinal tube wave energy fluxes and determined wave periods (see Table 1 and Paper I). To account for the energy carried by transverse tube waves (Huang et al. 1995; Musielak & Ulmschneider 2001b), the longitudinal wave fluxes were increased by a factor M , where for a realistic contribution we take $M = 5$. The waves were allowed to propagate in the constructed two-component atmosphere model (see Paper I), where they dissipate their energy by forming shocks. With a multi-ray transfer code described in Paper I, we then simulated line profiles of the Ca II H+K and Mg II h+k lines emerging from our theoretical chromospheric models and will now compare them with observations.

3.1. Mean temperatures in the flux tube models

Before discussing the emerging radiative fluxes, it is important to have a better understanding of the wave computations. As mentioned in Paper I, a magnetic flux tube is constructed by selecting f and using the fluxes and wave periods given in Table 1. Then, the time-dependent MHD wave computation are carried out until about 40 to 50 shocks are transmitted at the top boundary of the model. Figure 3 shows time-averaged temperatures in the tube models.

It is found that hot stars have a broad temperature minimum region and a gradual mean temperature rise, while in cool stars a narrow temperature minimum region with an abrupt onset of the chromospheric temperature rise is seen. This behavior is met in semi-empirical chromosphere models of Kelch (1978) and Kelch et al. (1979) and is similar to that found in our acoustic wave computations (Schmitz & Ulmschneider 1981; Buchholz et al. 1998, Fig. 6). It can be attributed to the fact that in the hot stars the radiation field is so intense that radiation damping strongly affects the amplitude growth of the waves. In this situation, first described by Ulmschneider et al. (1979), after formation, the shocks and consequently shock

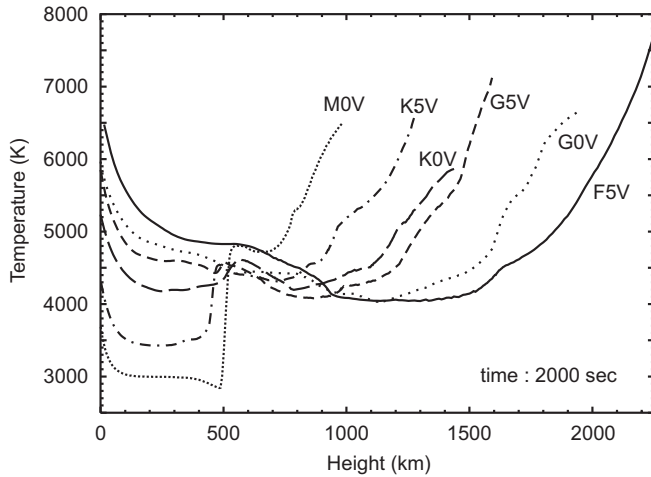


Fig. 3. Mean temperatures as function of heights for the sample of main sequence stars of filling factor $f = 0.1$.

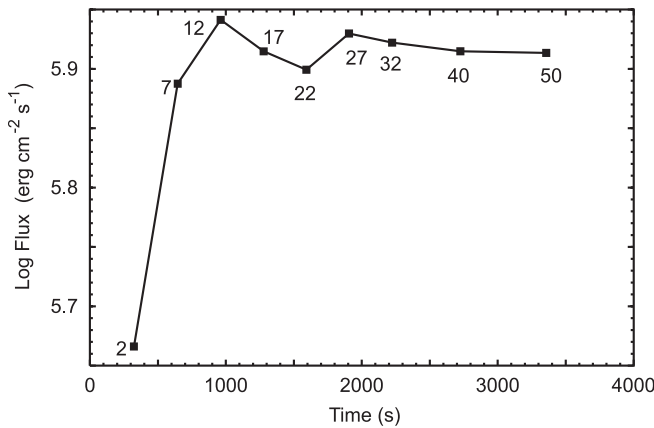


Fig. 4. The variation of the emitted Mg II h+k flux with time, for a G5V star of filling factor $f = 0.1$. The numbers indicate how many shocks have already gone through the atmosphere.

heating grow very little until they have left the radiation damping zone. In cool stars, where shock formation occurs outside this zone, shock heating sets in abruptly after shock formation. This latter effect is enhanced by our use of monochromatic waves which lets shocks form always near the same height. Here a somewhat less abrupt temperature rise could occur when a more realistic acoustic spectrum calculation is performed.

Similarly as in Buchholz et al. (1998), Fig. 3 for the K0V up to M0V models shows pronounced temperature plateaus, although these plateaus in our present work are lower and even show a slight outward decrease with height. The different plateau temperatures could be due to the fact that they here are for magnetic flux tubes while the outward decrease might be an artifact of our averaging process. The latter could also be a peculiarity of magnetic flux tubes where after fairly strong shocks have formed, they might suffer amplitude decreases over some height intervals in the exponentially spreading tubes before the constant cross-section regions are reached.

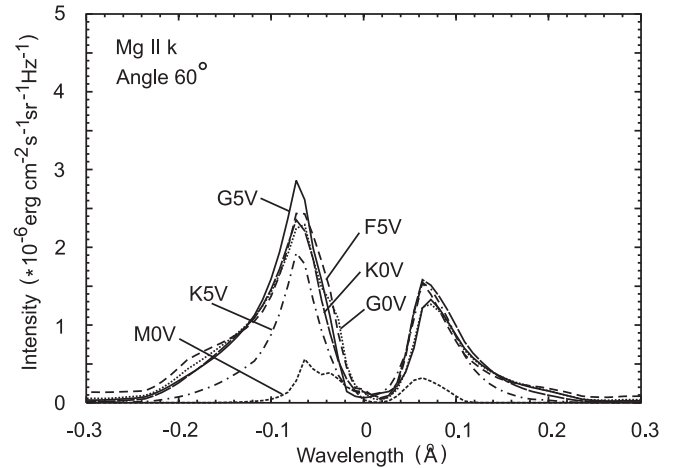


Fig. 5. Mg II k line profiles for main sequence stars of different spectral type, with a magnetic filling factor $f = 0.1$ and a multiplication factor $M = 0.5$, for an angle 60° .

That the wave calculations have to be carried out over sufficient time to ensure that the state of dynamical equilibrium has been reached is illustrated in Fig. 4. Here the development of the emergent total Mg II h+k line flux is seen as a function of time for a magnetic wave calculation in a G5V star with filling factor $f = 0.1$. Figure 4 shows that after the passage of about 40 to 50 shocks the emitted flux becomes stable.

3.2. Dependence on the filling factor

Comparison of Figs. 5 and 6 shows that the emergent radiative flux significantly increases with increasing magnetic filling factor. The reason for this is the increase in the number of flux tubes, which enlarges the total magnetic wave flux injected into the outer atmosphere (see Fig. 6 of Paper I). More heating in the magnetic flux tube forest occurs also because with high filling factors the wave energy is distributed over much narrower tube cross-sections which leads to stronger shocks (for details, see Fawzy et al. 1998). Note that as mentioned in Paper I, the displayed asymmetries of the red and violet emission peaks appear to be too large compared to observed ones, which may be due to our use of monochromatic waves. However, large asymmetries have also been observed (see Paper I).

It is important to point out that very high values of the magnetic filling factor close to one are not realistic for the wave heating picture. We believe that maximum wave heating is achieved for filling factors around $f = 0.4$. To understand this, we must keep in mind that the longitudinal and transverse tube wave generation critically depends on the free homogenous turbulence of the gas flow outside the magnetic flux tubes. In this situation, the main energy carrying bubbles have vertical sizes of the order of a scale height, and their horizontal diameters are typically larger than the vertical sizes.

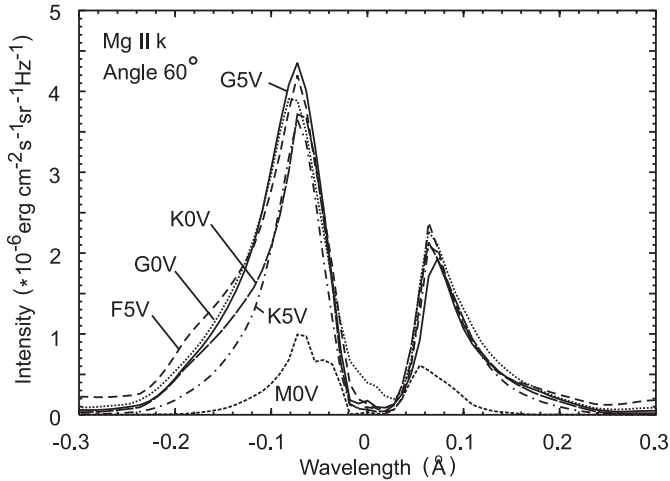


Fig. 6. The same as Fig. 5 but for magnetic filling factor $f = 0.4$.

This means that the situation becomes critical when the available space for the turbulent flows becomes smaller than a scale height, which is the case for filling factors greater than $f = 0.4$ (see Paper I). Increasing the filling factor above this value would critically reduce the space available for the convective bubbles and thus significantly decrease the efficiency of the generation of magnetic tube waves. Direct magnetic field dissipation might still increase in situations with higher filling factors. However, we then expect to get less heating by magnetic waves which are the main object of investigation in our present work.

Figure 7 shows the dependence of the total emerging flux in Ca II H+K on the magnetic filling factor. Also shown is the range of observed fluxes indicated by the lines “Min” and “Max” displayed in Fig. 2 and given by our Eq. (1). It is seen that for tiny filling factors, close to the value of $f = 0.02$ like on the Sun, one has only small contributions from the magnetic heating (see also Fawzy et al. 1998) and the theoretical energy flux is essentially due to acoustic heating. For higher values of f the theoretical emission fluxes increase. The variation of f seems to be sufficient to explain most of the stellar activity range between the observed limits. To be more precise, more than half of this gap can be explained for hot stars and essentially all of this gap is accounted for by our theory for cool stars. How significant this result is for the explanation of the chromospheric heating, in view of the expected errors of our method, will be discussed below.

3.3. Contribution from transverse tube waves to the heating

As mentioned above a realistic magnetic wave calculation must also consider the dissipation of transverse waves via nonlinear mode-coupling to longitudinal tube waves (Ulmschneider et al. 1991). Actually, we should also consider the generation of torsional waves; unfortunately, the efficiency of generation of these waves is currently not known (see, however, Hollweg et al. 1982;

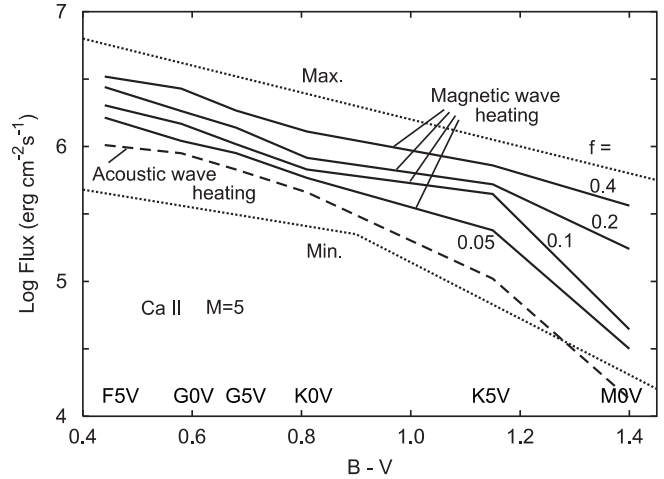


Fig. 7. Total Ca II H+K emission fluxes from late-type stars for different filling factors f with a multiplication factor $M = 5$. Min and Max indicate observational limits given by our Eq. (1).

Narain & Ulmschneider 1996). As we do not know how much of the transverse tube wave energy flux leaks out of stellar magnetic flux tubes (for some estimates, see Ziegler & Ulmschneider 1997; Huang et al. 1999), we assume that only a fraction of the generated transverse wave energy is actually converted into longitudinal wave energy.

In addition, there is the question where the transverse wave energy becomes available for longitudinal shock wave heating. Zhugzhda et al. (1995) have shown that longitudinal and kink shocks occur at the same height despite of the different propagation speeds of the two wave modes. As a result, transverse wave energy becomes available by nonlinear mode-coupling when longitudinal shocks form. One also expects strong nonlinear mode-coupling at greater heights, where adjacent flux tubes meet one another and transverse motions will generate compressions in the gas squeezed between the neighboring field lines. This may actually give rise to spicules (see e.g. Cheng 1992). Obviously, questions of this type can only be answered after more elaborate three-dimensional MHD simulations of magnetic flux tubes become available.

As discussed above, a crude way to study the influence of mode-coupling on the magnetic wave heating is to simply increase the longitudinal tube wave fluxes F_L given in Table 1 by the amount provided from transverse waves in using a flux multiplication factor M , for which we might take values up to $M = 10$. This is because these waves are generated with factors of 10 to 30 greater efficiency compared to longitudinal tube waves (see Huang et al. 1995; Musielak & Ulmschneider 2001, 2002). A maximum factor $M = 5$ is taken in our present work, however, because of the unknown amount of leakage of transverse waves.

Figure 8 shows the total Ca II H+K emission fluxes obtained when transverse wave heating is taken into account. The figure displays the results for different multiplication factors M using the maximum filling factor of $f = 0.4$. Here “Min” and “Max” indicate the observed range of chromospheric emission displayed in Fig. 2 and

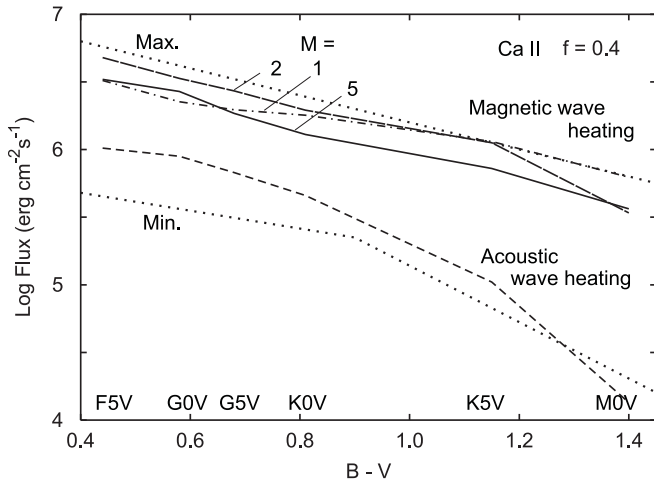


Fig. 8. Surface averaged Ca II H+K fluxes from late-type stars vs. $B - V$ for different longitudinal wave fluxes MF_L , with indicated multiplication factors M , for two-component model atmospheres, with a filling factor $f = 0.4$. Min and Max denote observational limits given by our Eq. (1).

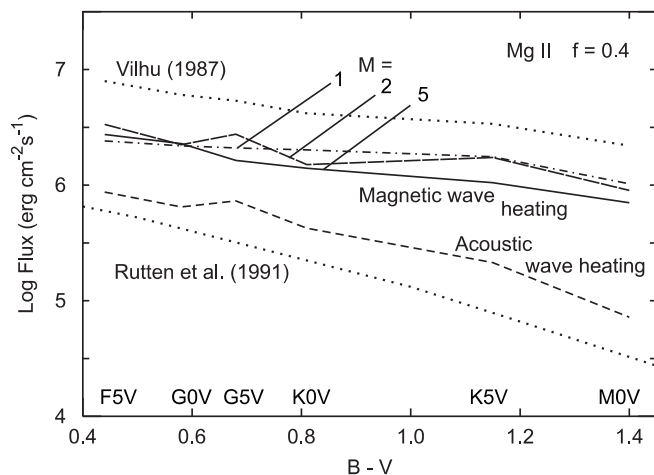


Fig. 9. The same as Fig. 8 however for Mg II. Also shown are observational limits by Rutten et al. (1991) and Vilhu (1987).

Eq. (1). The similar case for the total Mg II h+k emission fluxes is shown in Fig. 9 where the observational limits are given by the Rutten et al. (1991) and Vilhu (1987).

Both figures show that the increase of $M = 1$ to $M = 5$ does not affect much the chromospheric emission. This can be explained by the fact that in the slender flux tubes with filling factor $f = 0.4$ the limiting strength property has set in (see Ulmschneider 1991; Fawzy et al. 1998). This property leads to similar shaped shocks and shock heating. As the limiting strength is independent of the initial wave flux, the heating becomes insensitive to the input flux. However, when large wave fluxes are dissipated in the low atmosphere regions where the tubes expand and the limiting strength property has not yet set in, we expect that the scale height will be affected and a much reduced influence on the emergent radiative flux will remain.

That the fluxes with $M = 1$ to 5 are so different in Figs. 8 and 9 is caused primarily by the fact that for the

cases $M = 1$ and $M = 2$ the wave calculations were carried out only to between 33 and 40 shock transmissions instead of the 50 transmissions for the case $M = 5$. The differences thus show the variations associated with the atmospheric oscillations following the onset of the wave calculation. At this point we have to note that after 50 shock transmissions, our chromosphere models have reached a stable dynamical equilibrium which may be an artifact of our monochromatic wave calculation. In realistic situations where one has an acoustic wave spectrum such quiet dynamical states would not occur and the atmosphere would continue to pulsate aperiodically. This suggests that the differences between the cases $M = 1$ to 5 give an indication of the possible range of the magnetic wave heating in excess of the quiet case $M = 5$. Because of this, the variation of the emission flux with the filling factor appears to be large enough to cover most of the observed range of the chromospheric emission fluxes between the observational limits.

At this point, we must say that varying M serves only as means to display the influence of different amounts of transverse wave energy available for the heating. Note that in the tightly packed field configuration, with filling factors $f = 0.4$, the efficiency of nonlinear mode-coupling will be high and, therefore, the choice of $M = 5$ is very likely a lower estimate in view of the fact that transverse waves are much more efficiently generated, and that the leakage in such a tightly packed flux tube forest cannot be very large. In addition, the torsional wave contribution is missing altogether, and it is obvious that any leaked wave energy can hardly vanish without a trace, but instead must be involved in heating the local medium and the driving of spicules. Also it has to be noted that the limiting shock strength property will be locally superseded when additional wave flux is added at great height.

3.4. Can wave heating explain the chromospheric activity?

We now want to address the question of the importance of the magnetic wave heating and compare our calculated radiative fluxes with observations from individual stars. To judge the significance of this comparison it should be recalled that *the theoretical emission fluxes were computed completely based on first principles*, specifying for our stars only the 4 parameters T_{eff} , g , metallicity Z_M (solar), and f . Our theoretical computations thus carry all the accumulated systematic errors of the wave flux generation calculations, the chromospheric wave modelling and the radiation treatments. If our chosen mechanisms for heating the outer stellar atmospheres were completely unrealistic, or even if this heating were only a minor contribution, we would expect *large discrepancies* between our theoretical results and the observations.

In Figs. 10 and 11 our total theoretical Ca II H+K and Mg II h+k emission fluxes are compared with the observed emission fluxes from individual low and high activity stars

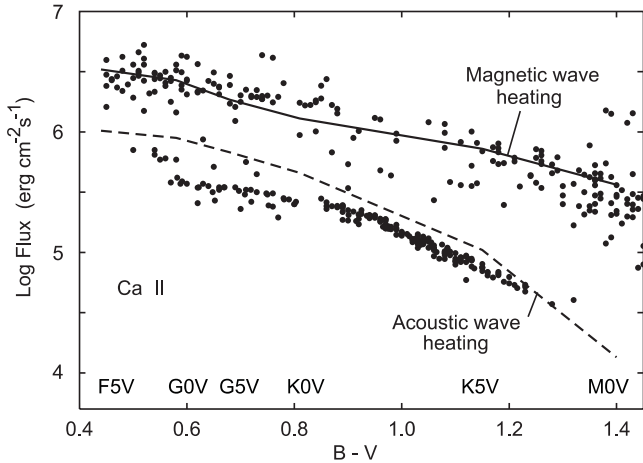


Fig. 10. Total observed Ca II H+K line core emission fluxes (with subtracted photospheric background) of minimum flux stars and most active dwarfs are shown as dots, compared with theoretical fluxes for pure acoustic wave heating (dashed) and for magnetic wave heating in flux tubes, which at photospheric height have an area filling factor of $f = 0.4$ with $M = 5$ (solid).

discussed in Sect. 2. For our calculations, we used fluxes with $M = 5$ and filling factors $f = 0.4$, which corresponds to the case of the most efficient magnetic wave heating. It should be noted that our stellar chromospheric models are normally two-component models, hence, the displayed models labeled acoustic wave heating and magnetic wave heating represent only the limiting cases. Namely, acoustic wave heating represents models with the filling factors $f = 0$, that is, no magnetic flux tubes are considered, while for magnetic wave heating we have models with $f = 0.4$, which means that the stellar surface is almost completely covered by narrow intensely heated magnetic flux tubes, and the external acoustic heating component is present but turns out to be negligible. It should also be mentioned that Figs. 10 and 11 as well as most figures in this paper represent recent recomputations extending the wave calculations to 50 wave periods and taking the core fluxes between 0.95 \AA . These figures are therefore slightly different from the work published by Ulmschneider et al. (2001a).

a. The Ca II emission fluxes

Figure 10 shows that the observational range of the Ca II H+K line emission fluxes is about an order of magnitude for hot stars and almost two orders of magnitude for cool stars. It is seen that the theoretical magnetic wave heating line agrees more or less (given the uncertainties) with the observed stars with maximum chromospheric emission. We estimate that the uncertainty of the theoretical Ca II fluxes is at least a factor of two. This is because of a number of reasons: the atmospheric oscillations, that only four wave phases were taken for our average, the uncertainty about the multiplication factor, as well as the fact that mode-coupling will provide longitudinal wave energy precisely at greater heights where the Ca II emission originates.

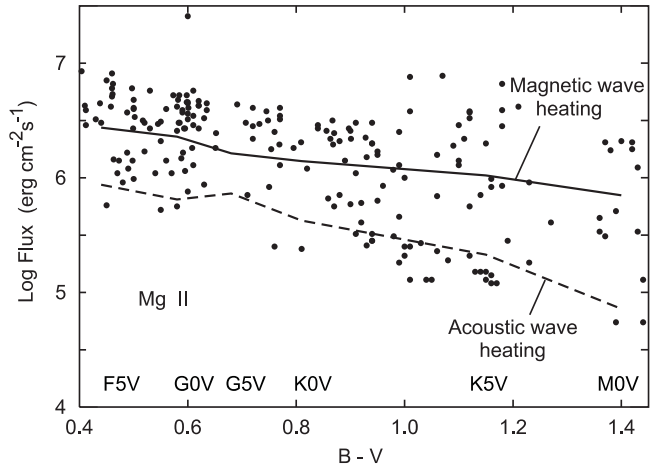


Fig. 11. Total observed Mg II h+k line emission of stars by Vilhu (1987) and Rutten et al. (1991) (dots), compared with theoretical fluxes for pure acoustic wave heating (dashed) and for magnetic wave heating in flux tubes, which at photospheric height have an area filling factor of $f = 0.4$ (solid).

At the low emission boundary the theoretical acoustic wave heating line lies a factor of about two above the observations for hot stars while agreeing well with cool stars. Here we have to recall that different to magnetic waves which have a much lower velocity dependence (see Ulmschneider et al. 2001b) the acoustic waves are generated by quadrupole sound generation, which according the Lighthill-Stein theory depends on the 8th power of the convective velocity v . As already noted in Paper I, we find sharply peaked convective velocity maxima v_{\max} that are unrealistically close to the local sound speed; clearly, the Lighthill-Stein theory becomes unreliable in these circumstances and a considerable overestimate of the generated acoustic fluxes for these stars is very likely (see also Stepień 1988).

In addition, it must be noted that the observed minimum fluxes for hot stars are determined with the lowest accuracy because the photospheric background flux in these stars is equal to roughly 90% of the total observed flux (see Figs. 1 and 2) and that the uncertainties among different $F_{\text{phot}}(B - V)$ increase with decreasing $B - V$. A set of radiative equilibrium models with appropriate values of $B - V$ and $\log g$ is needed to determine accurately the photospheric background flux in these stars. Clearly this also applies to our theoretical fluxes, where by subtracting a photospheric background based on the crude initial atmosphere models of Fig. 5 of Paper I we generate large errors.

Despite these inaccuracies, we find that the considered wave heating can in principle account for the observed chromospheric Ca II line-core emission fluxes, both in terms of the absolute flux as function of spectral type and the variability caused by different area filling factors of the magnetic field coverage.

b. The Mg II emission fluxes

Figure 11 shows the observed emission fluxes in the Mg II h+k lines for late-type stars taken from Vilhu (1987)

and Rutten et al. (1991). Similarly as for the Ca II fluxes, it is seen that the observed minimum flux limit agrees within about a factor of two with the emission flux of non-magnetic stars that are heated purely by acoustic waves (see also Buchholz et al. 1998). However, the magnetic wave heating for our stars with largest filling factors ($f = 0.4$), even taking a factor of two uncertainty into account, appears to be systematically below the maximum observed emission limit. Although most of the observed variability of the chromospheric emission appears to be covered by varying f , this gap seems to persist, independently of the effective temperature. As the Mg II h+k lines are formed higher in the atmosphere than the Ca II H+K lines, this suggests that one probably needs additional magnetic heating.

One possible candidate obviously is *torsional magnetic waves*. However, as we do not know how efficiently these are produced and how strongly and at what height they dissipate, we must await future investigations. It could well be that the behaviour of the torsional waves is similar to the transverse waves and that they form switch-on shocks (Hollweg et al. 1982) which might coincide with longitudinal shocks thus leading to strong nonlinear mode-coupling. If our method to increase the longitudinal flux F_L by a multiplication factor M is adequate, then, the inclusion of torsional waves would simply mean to increase M above our current maximum value 5. If the nonlinear mode-coupling between torsional and longitudinal tube waves would occur preferentially at great heights, additional wave heating would indeed improve the agreement with the Mg II observations. Unfortunately we know very little about torsional tube wave heating.

Another even more likely way to increase the theoretical Mg II maximum emission fluxes is by including a *non-wave heating mechanism* that operates at great heights. Here, reconnective heating by microflares seems to be a very attractive candidate (see Narain & Ulmschneider 1996). That this indeed might be the case is also suggested by observations of the line widths of stellar C IV transition-layer lines observed by Wood et al. (1997). In addition Mitra-Kraev & Benz (2001) have shown that the observed extreme ultraviolet (EUV) and X-ray emission fluxes from the quiet solar corona can be successfully described by a nanoflare heating model.

The following scenario of chromospheric heating emerges from our results: the base of stellar chromosphere is heated by pure acoustic (shock) waves, the heating of the middle and upper chromospheric layers is dominated by magnetic waves associated with magnetic flux tubes, and that other non-wave heating mechanisms (e.g., reconnection) seem to be required to explain the structure of the highest layers of stellar chromospheres.

4. Conclusions

We have compared the observed chromospheric emission fluxes in the Ca II H+K and Mg II h+k lines of late-type main sequence stars with our theoretical results.

The theoretical calculations were based completely on first principles, that is, we specify only the four independent stellar parameters: effective temperature T_{eff} , gravity g , metallicity Z_M (we took solar-like population I metal abundances), and magnetic filling factor f at the stellar surface. With these four parameters, which uniquely identify a star, we constructed stellar convection zone models and theoretical, time-dependent, two-component models of stellar chromospheres. The models consist of non-magnetic regions heated by acoustic waves and magnetic flux tube regions heated by magnetic tube waves. The magnetic field in these models occurs mainly in the form of thin flux tubes, which at the stellar surface have diameters equal to the local scale height. The magnetic field strength at this height is assumed to be given by a fixed fraction of the equipartition field strength, which is determined by the external gas pressure.

Using the Lighthill-Stein theory for the generation of acoustic waves and a numerical method for the generation of magnetic tube waves, we have calculated acoustic and longitudinal wave fluxes and determined wave periods. To take into account transverse waves, the longitudinal wave fluxes were increased by a factor M , where for a realistic contribution we took $M = 5$. These waves were allowed to propagate in stellar chromospheres described by our theoretical model and dissipate their energy by forming shocks. With a multi-ray transfer code we have simulated line profiles of the Ca II H+K and Mg II h+k lines emerging from our theoretical chromospheric models and compared them with observations. The following conclusion can be drawn from this comparison:

1. The theoretical emission fluxes in the Ca II and Mg II lines computed from our chromospheric models based exclusively on acoustic and magnetic wave heating agree relatively well with the observed ones, both in terms of the absolute magnitude and in terms of the T_{eff} -dependence.
2. The variability of the chromospheric emission observed for stars of different rotation rates but similar gravity and T_{eff} can be explained by the different amount of magnetic wave heating caused by the variation of the magnetic filling factor f . For small filling factors, pure acoustic wave heating explains the minimum chromospheric emission, the so-called “basal flux”. Very large filling factors ($f = 0.4$), in addition to acoustic heating, lead to intense and dominant magnetic wave heating, which provides full explanation of the maximum emission (“saturation” limit) observed in the Ca II lines and partial explanation of the observed maximum emission in the Mg II lines.
3. The conspicuous gap between the maximum emission generated by magnetic wave heating and the observed “saturation” limit in the Mg II lines can be attributed to the greater formation height of these lines (compared to Ca II) and appears to indicate that an additional non-wave heating mechanism is needed to account for the structure of these highest chromospheric layers.
4. A coherent picture of the heating of the outer atmospheres of late-type stars appears to be emerging.

Turbulent gas motions in the surface convection zones of these stars give rise to acoustic waves, and working on the thin magnetic flux tubes, to longitudinal and transverse magnetic waves. These waves steepen into shock waves, heat the outer atmosphere and produce chromospheres.

We finally conclude that in late-type stars the base of the chromosphere is heated by acoustic waves, while in the middle and upper chromosphere the heating is dominated by magnetic waves in flux tubes. In the highest chromospheric layers, at the foot of the transition region and in the corona, an additional non-wave heating mechanism is required. A very likely candidate for this mechanism is reconnective (microflare) heating.

Acknowledgements. This work was supported by NSF under grant ATM-0087184 (Z.E.M. and P.U.), by the KBN grant 5 P03D 006 21 (K.S.), by the DFG grants Ul57/25-3, Ul57/30-1 and by NATO under grant CRG-910058 (P.U. and Z.E.M.). Z.E.M. also acknowledges the support of this work by the Alexander von Humboldt Foundation.

References

- Blanco, C., Catalano, S., Marilli, W., & Rodono, M. 1974, *A&A*, 33, 257
- Buchholz, B., Ulmschneider, P., & Cuntz, M. 1998, *ApJ*, 494, 700
- Cheng, Q. Q. 1992, *A&A*, 226, 549
- Doyle, J. G., Short, C. I., Byrne, P. B., & Amado, P. J. 1998, *A&A*, 329, 229
- Duncan, D. K., Vaughan, A. H., Wilson, O. C., et al. 1991, *ApJS*, 76, 383
- Dupree, A. K., Hartmann, L., & Smith, G. H. 1990, *ApJ*, 353, 623
- Dupree, A. K., Whitney, B. A., & Pasquini, L. 1999, *ApJ*, 520, 751
- Durney, B. R., & Latour, J. 1978, *Geophys. Astrophys. Fluid Dyn.*, 9, 241
- Fawzy, D. E., Rammacher, W., Ulmschneider, P., Musielak, Z. E., & Stepień, K. 2002, *A&A*, 386, 971 (Paper I)
- Fawzy, D. E., Ulmschneider, P., & Cuntz, M. 1998, *A&A*, 336, 1029
- Flower, P. J. 1996, *ApJ*, 469, 355
- Hall, J. C., & Lockwood, G. W. 1995, *ApJ*, 438, 404
- Henry, T. J., Soderblom, D. R., Donahue, R. A., & Baliunas, S. L., 1996, *AJ*, 111, 439
- Hollweg, J. V., Jackson, S., & Galloway, D. 1982, *Solar Phys.*, 75, 35
- Huang P., Musielak, Z. E., & Ulmschneider, P. 1995, *A&A*, 279, 579
- Huang P., Musielak, Z. E., & Ulmschneider, P. 1999, *A&A*, 342, 300
- Kelch, W. L. 1978, *ApJ*, 222, 931
- Kelch, W. L., Worden, S. P., & Linsky, J. L. 1979, *ApJ*, 229, 700
- Lighthill, M. J. 1952, *Proc. Roy. Soc. London A*, 211, 564
- Linsky, J. L., Worden, S. P., McClintock, W., & Robertson, R. M. 1979, *ApJS*, 41, 47
- Mathioudakis, M., & Doyle, J. G. 1992, *A&A*, 262, 523
- Mauas, P. D. J., Falchi, A., Pasquini, L., & Pallavicini, R. 1997, *A&A*, 326, 249
- Mewe, R., Schrijver, C. J., & Zwaan, C. 1981, *Space Sci. Rev.*, 30, 191
- Mermilliod, J.-C. 1994, *Bull. Inf. CDS*, 45, 3
- Middelkoop, F. 1982, *A&A*, 107, 31
- Mitra-Kraev, U., & Benz, A. O. 2001, *A&A*, 373, 318
- Musielak, Z. E., Rosner, R., Stein, R. F., & Ulmschneider, P. 1994, *ApJ*, 423, 474
- Musielak, Z. E., & Ulmschneider, P. 2001, *A&A*, 370, 541
- Musielak, Z. E., & Ulmschneider, P. 2002, *A&A*, 386, 606
- Narain, U., & Ulmschneider, P. 1996, *Space Sci. Rev.*, 75, 453
- Noyes, R. W., Hartmann, L. W., Baliunas, S. L., Duncan, D. K., & Vaughan, A. H. 1984, *ApJ*, 279, 763
- Rutten, R. G. M. 1987, *A&A*, 177, 131
- Rutten, R. G. M., Schrijver, C. J., Lemmens, A. F. P., & Zwaan, C. 1991, *A&A*, 252, 203
- Saar, S. H. 1994, in *Infrared Solar Physics*, ed. D. M. Rabin, J. T. Jefferies, & C. Lindsey (Kluwer, Dordrecht), 493
- Saar, S. H. 1996, in *IAU Symp. 176, Stellar Surface Structure*, ed. K. Strassmeier, & J. L. Linsky (Kluwer Academic Publ.), 237
- Schmitz, F., & Ulmschneider, P. 1981, *A&A*, 93, 178
- Schrijver, C. J. 1983, *A&A*, 127, 289
- Schrijver, C. J. 1987, *A&A*, 172, 111
- Schrijver, C. J., Coté, J., Zwaan, C., & Saar, S.H. 1989, *ApJ*, 337, 964
- Soderblom, D. R., Duncan, D.K., & Johnson, D. R. H. 1991, *ApJ*, 375, 722
- Stein, R. F. 1967, *Solar Phys.*, 2, 385
- Stepień, K. 1988, *ApJ*, 335, 892
- Stepień, K. 1989, *A&A*, 210, 273
- Stepień, K. 1993, in *The Cosmic Dynamo*, ed. F. Krause, K. H. Radler, & G. Rüdiger (Kluwer, Dordrecht), 141
- Stepień, K. 1994, *A&A*, 292, 191
- Strassmeier, K. G., Fekel, F., Bopp, B. W., Dempsey, R. C., & Henry, G. W. 1990, *ApJS*, 72, 191
- Strassmeier, K. G., Handler, G., Paunzen, E., & Rauth, M. 1994, *A&A*, 281, 855
- Ulmschneider P. 1991, in *Mechanisms of Chromospheric and Coronal Heating*, ed. P. Ulmschneider, E. Priest, & R. Rosner (Springer Verlag, Berlin), 328
- Ulmschneider, P., Fawzy, D. E., Musielak, Z. E., & Stepień, K., 2001a, *ApJ*, 559, L167
- Ulmschneider, P., & Musielak, Z. E. 1998, *A&A*, 338, 311
- Ulmschneider, P., Musielak, Z. E., & Fawzy, D. E. 2001b, *A&A*, 374, 662
- Ulmschneider, P., Schmitz, F., & Hammer, R. 1979, *A&A*, 74, 229
- Ulmschneider, P., Theurer, J., & Musielak, Z. E. 1996, *A&A*, 315, 212
- Ulmschneider, P., Zähringer, K., & Musielak, Z. E. 1991, *A&A*, 241, 625
- Vaughan, A.H., & Preston, G. W. 1980, *PASP*, 92, 385
- Vilhu, O. 1987, in *Cool Stars, Stellar Systems, and the Sun*, ed. J. L. Linsky, & R. E. Stencel (Springer, Berlin), 110
- Vilhu, O., & Walter F. M. 1987, *ApJ*, 321, 958
- Wilson, O. C. 1968, *ApJ*, 153, 221
- Weiss, N. O. 1994, *Lectures on Solar and Planetary Dynamoes*, M. R. E. Proctor, & A. D. Gilbert (Cambridge Univ. Press), 59
- Wood, B. E., Linsky, J. L., & Ayres, T. R. 1997, *ApJ*, 478, 745
- Zhugzhda, Y., Bromm, V., & Ulmschneider, P. 1995, *A&A*, 300, 302
- Ziegler, U., & Ulmschneider, P. 1997, *A&A*, 327, 854